Long-term variations of the electron slot region and global radiation belt structure

Shing F. Fung,[1] Xi Shao,[1,2] and Lun C. Tan[1,3]

[1]   We report the observations of changes of the nominal position of the quiet-time radiation belt slot over the solar cycles. It has been found that the slot region, believed to be a result of enhanced precipitation losses of energetic electrons due to their interactions with VLF waves in the magnetosphere, tends to shift to higher L ($\sim$3) during a solar maximum compared to its canonical L value of $\sim$2.5, which is more typical of a solar minimum. The solar-cycle migration of the slot can be understood in terms of the solar-cycle changes in ionospheric densities, which may cause the optimal wave-particle interaction region during higher solar activity periods to move to higher altitudes and higher latitudes, thus higher L. Our analysis also suggests that the primary regions of wave-particle interaction processes that result in the slot formation are located off of the magnetic equator. Citation: Fung, S. F., X. Shao, and L. C. Tan (2006), Long-term variations of the electron slot region and global radiation belt structure, *Geophys. Res. Lett.*, *33*, L04105, doi:10.1029/2005GL024891.

1.   Introduction

[2]   The Van Allen radiation belts are permanent features of Earth's inner magnetosphere, although their structures are known to vary with geomagnetic activities. Subsequent to the main phase of a storm, the electron slot region, believed to result from losses of trapped electrons caused by precipitation induced by pitch-angle scattering by VLF waves in the plasmasphere, can be completely filled with energetic electrons, leading to the disappearance of the slot and the overall enhancement of the outer-belt electron fluxes. The slot then recovers after the storm has decayed sufficiently, typically a few days after the main phase. The slot region, nominally located at $2 < L < 3$, thus is a salient feature of the radiation belts, separating the inner and outer belts.

[3]   Due to the potential hazards of energetic electrons on space systems, radiation-belt studies have focused on the source mechanisms that might lead to enhancements of energetic electron fluxes. Much less attention has been paid to the particle loss mechanisms or the slot region. The processes involved in the creation of the slot, however, are connected intimately to the decay of a geomagnetic storm. Understanding the development and maintenance of the slot, i.e., processes leading to the production of

VLF waves in the slot L range, are therefore important for delineating the physics of post-storm magnetospheric dynamics.

[4]   We have investigated the solar-cycle behavior of the electron slot region in order to elucidate the magnetospheric conditions controlling the long-term slot structure. The main topic of this paper is to describe the apparent shifts of the slot region observed at low altitudes ($\sim$850 km) by different NOAA satellites over the solar-cycle time scale [*Fung et al.*, 2005], and investigate the probable cause of that shift due to changes in ionospheric densities and the VLF wave pattern at high altitudes.

2.   Formation of the Quiet-Time Electron Slot Region

[5]   It is generally known that the radiation belt slot region is formed by losses of energetic electrons by enhanced pitch-angle scattering by VLF waves, most likely whistler waves associated with plasmaspheric hiss emission [e.g., *Lyons and Thorne*, 1973; *Lyons and Williams*, 1984; *Imhof et al.*, 1982]. There have been many discussions, however, on the sources and distributions of the waves responsible for the electron scattering in the slot [e.g., *Abel and Thorne*, 1998a, 1998b; *Imhof et al.*, 1986; *Bortnik et al.*, 2002, 2003; *Green et al.*, 2005a, 2005b]. It is remarkable that they all seem to predict the canonical position of the slot ($2 < L < 3$), making it difficult to observationally distinguish the dominant slot formation process.

[6]   *Abel and Thorne* [1998a, 1998b] conducted relatively extensive studies of pitch angle diffusion and calculated electron precipitation lifetimes resulting from various scattering processes due to Coulomb interactions with thermal plasma, plasmaspheric hiss, lightning-generated whistlers, and VLF transmitter waves. They found that the slot occurrence is basically accounted for by some appropriate combinations of the various scattering processes. They also found, however, that these processes can also be affected by the average propagation characteristics of the scattering waves. As the plasma and wave characteristics are likely to be affected by magnetospheric conditions, it is then of interest to determine the quiet-time equilibrium structure of the slot without the transient effects of dynamical processes, so that the "ground-state" structure of the radiation belt structure can be ascertained.

3.   Solar-Cycle Variations of the Electron Slot Region

[7]   Except during strong storms when the slot region can be filled temporarily or new belts can form, the slot is a salient feature of the Van Allen radiation belts, most

---

[1]Space Physics Data Facility, NASA Goddard Space Flight Center, Greenbelt, Maryland, USA.
[2]Formerly at NAS National Research Council, Washington, DC, USA.
[3]QSS Group, Inc., Lanham, Maryland, USA.
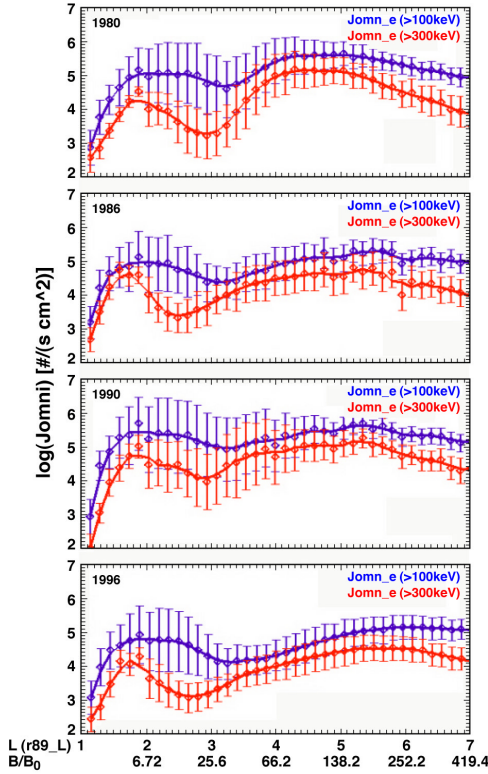
Figure 1. L-B/B_0 profiles of quiet-time ($Kp \leq 2$ and $Vsw \leq 400$ km/s) omnidirectional electron fluxes [>100 keV (in blue) and >300 keV (in red)] measured by MEPED [*Raben et al.*, 1995] aboard the NOAA 5, 6, 7, 8, 10, and 12 satellites during June, July and August in solar maximum (1980, 1990) and solar minimum (1986, 1996) years. A shift in the slot location between solar minimum and solar maximum is clearly seen at >300 keV.

noticeable during geomagnetically quiet times. While most radiation belt studies tend to focus on the outer or inner belt [e.g., *Li et al.*, 2001; *Friedel and Korth*, 1995; *Miyoshi et al.*, 2004], long-term variations of the quiet-time slot region have received much less attention. Since the slot region is relatively devoid of hazardous radiation fluxes and can present a safe zone for Earth orbiting satellites, we need to examine if there exist any long-term variations of the slot that may shed light on the maintenance of the global radiation belt structures.

[8] *Fung et al.* [2005] show recently that there is a noticeable shift in the average slot location from $L \sim 2.5$ during solar minimum to $L \sim 3$ during solar maximum. A similar shift is noted by *Green et al.* [2005a]. Figure 1 shows the L-B/B_0 profiles of omnidirectional electron fluxes observed during geomagnetically quiet times in the months of June, July and August of 1980 and 1990 for solar maximum, and of 1986 and 1996 for solar minimum. The particle observations were obtained by the Medium Energy Proton Electron Detectors (MEPED) [*Raben et al.*, 1995] aboard different polar-orbiting, low-altitude NOAA satellites. The quiet intervals were obtained by using the Magnetospheric State Query System (MSQS, ⟨radbelts.gsfc.nasa.gov/RB_model_int/Psi_database.html⟩) [*Fung*, 2004a] for the conditions of $K_p \leq 2$ and solar wind speeds ≤ 400 km s^{-1}.

[9] As shown clearly in the energetic electron (>300 keV) observations in Figure 1, there is an apparent shift in the nominal slot location between higher and lower L as the solar cycle phase changes from solar maximum to solar minimum condition, and vice versa. While a slot-like feature is seen at lower energies (>100 keV), no apparent solar cycle-phase shift is seen in the less energetic electron observations. This is because the lower energy electrons are (1) more susceptible to the variability effects of magnetospheric electric fields and (2) less effectively scattered by plasmaspheric hiss (whistler) waves with frequencies >few 100 Hz [e.g., *Abel and Thorne*, 1998a, 1998b].

[10] Figure 2 shows the count rates, instead of omnidirectional fluxes, observed by the NOAA satellites in three consecutive years during a solar maximum (1979, 1989, and 1981) and solar minimum (1984, 1985, and 1986) period. Again to avoid effects of Earth rotation axis orientation variations, only observations from the same months: May, June and July from each year are plotted. The consistency in the quiet-time slot locations in the three consecutive years in a given solar cycle phase (solar minimum or solar maximum) is striking. The shift in the slot locations due to solar cycle changes, however, is quite apparent in the >300 keV observations. Figure 2 also shows that the slot at lower energies tends to occur at higher L, although they are much less affected by solar cycle phases.

[11] Solar-cycle variations of the quiet-time minimum electron flux (>300 keV) and its location in the slot are shown in Figure 3. The data are all taken in the months of June, July, and August during each year except that in 1988, the data is taken from the entire year since NOAA 10 has
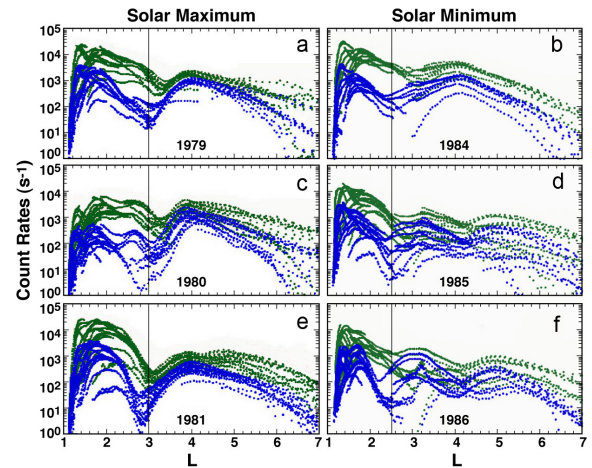
Figure 2. Radiation belt electron count rates at >100 (green) and >300 (blue) keV observed at low altitudes (at $0.55L^{3.29} < B/B_0 < 0.65L^{3.29}$) by the MEPED aboard the NOAA TIROS 5, 6, 7, and 8 satellites during quiet conditions ($K_p < 2$ and solar wind speeds < 400 km s^{-1}) in the months of May, June and July of three consecutive years during the (left) solar maximum and (right) solar minimum periods. The quiet-time slot feature is best seen in the energetic electron data (>300 keV, blue). The black vertical lines indicate the nominal slot positions in L. A small shift in the slot location ($\Delta L \sim 0.5$) is apparent between the two solar cycle phases (similar to Figure 4 in *Fung et al.* [2005], with permission from Elsevier).
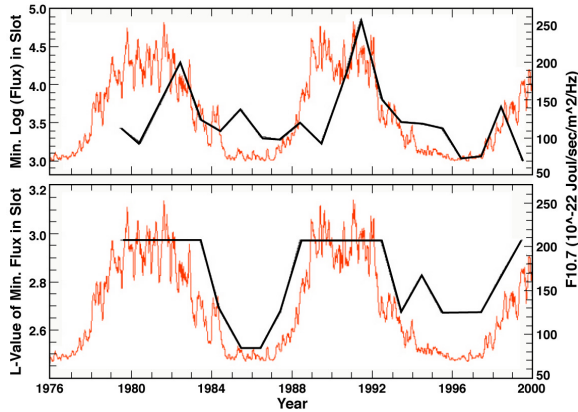
Figure 3. (top) Solar-cycle variations of the minimum flux in the slot region and (bottom) the L-value of minimum flux for energetic electrons (>300 keV) during quiet-time conditions (see Figure 1). The data are taken by NOAA 5, 6, 7, 8, 10, 12, and 14 during different intervals in the months of June, July, and August of each year. For 1988, however, the data is taken from the entire year since only NOAA 10 data are available, but with poor coverage during those months.

poor coverage. The quiet time intervals were again obtained by using the MSQS as above. As seen from Figure 3 (bottom) the slot minimum flux L value correlates nearly perfectly with solar activity. On the other hand, Figure 3 (top) shows that the slot minimum flux reaches a relative minimum near the beginning of the rising phase of a solar cycle, and it tends to maximize at the beginning of the declining phase of the solar cycle.

4. Discussions

[12] The quiet-time slot structures (Figure 3) found in this paper represent the equilibrium states of the radiation belt slot during solar maximum and solar minimum conditions, when all transient effects have subsided. While it may be expected that similar pitch angle scattering processes are responsible for the creation of the slot during different solar cycle phases, the degree to which the slot is evacuated and the primary location of the electron-loss processes are apparently solar-cycle dependent.

[13] From the results shown in Figures 1–3, it can be inferred that the primary site of precipitation losses of energetic electrons (>300 keV), hence the slot, must shift from $L \sim 2.5$ to slightly higher L (to ~3) as solar activity level changes from a minimum to a maximum. This seemingly oscillatory motion of the slot appears cyclical and is nearly in-phase with the 11-year solar cycle. This strong correlation between the slot position in L and solar activity suggests that the distributions of the whistler waves responsible for scattering and of the energetic electrons being scattered must somehow be controlled by the ionospheric density, which is higher and has a larger scale height during solar maximum than solar minimum [e.g., *Jursa*, 1985].

[14] As shown in Figures 1 and 2, the outer-belt energetic electron (>300 keV) distributions during solar minimum (quiet) conditions tend to be broader in L and have less

well-defined peaks. In addition, there appears to be shifts of the outer-belt flux peaks in L between solar cycle phases. But the distribution in 1984 (Figure 2b) does show evidence of an outer-belt peak location that is consistent with those observed during solar maximum, such as in 1979 (top Figure 2a). The inner-belt peak location ($L \sim 1.8$ for >300 keV) is relatively insensitive to solar cycle phase variations. Therefore, the observed shift of the slot as a function of solar cycle phase may not likely be due to any major shifts in the spatial distributions of trapped electrons in the radiation belts, but is probably due to the shifts in the scattering wave distributions.

[15] It may be instructive to consider how increases in ionospheric densities and scale heights during a solar activity maximum may lead to shifting of the slot to higher L values. Figure 4 shows a schematic of a given density level ($N = N_f$) during a solar minimum (inner dashed contour) and a solar maximum (outer dotted contour) superposed over the Earth's magnetic field (solid lines). Points A and B are the sites where precipitation losses of energetic electrons are effective due to pitch angle scattering by waves in a solar minimum and solar maximum period, respectively.

[16] For VLF waves that are effective in pitch angle scattering the slot electrons [e.g., *Abel and Thorne*, 1998a, 1998b; *Bortnik et al.*, 2002; *Green et al.*, 2005a, 2005b], their propagations are mediated by the background magnetized plasma that is generally characterized by its electron plasma frequency ω_{pe} and gyro frequency Ω_{ce}. In fact, for quasi-longitudinal propagation, the whistler mode dispersion relation is $n^2 \approx \omega_{pe}^2 / |\omega\Omega_{ce} \cos \theta|$, where n is the refractive index and θ is the wave normal angle [*Stix*, 1992]. Therefore, if waves having angular frequencies ω and propagation directions θ are effective in scattering energetic electrons in a region with a specific ratio of $\omega_{pe}^2/\Omega_{ce}$ ($\sim N/B$, where N is the local electron density and B is the magnetic field strength), then that characteristic frequency ratio defines the region of enhanced precipitation losses.

[17] Based on the above scenario, it is easy to imagine that the region of enhanced precipitation corresponds to region A in Figure 4 during solar minimum, when the overall ionospheric electron densities are lower. Due to
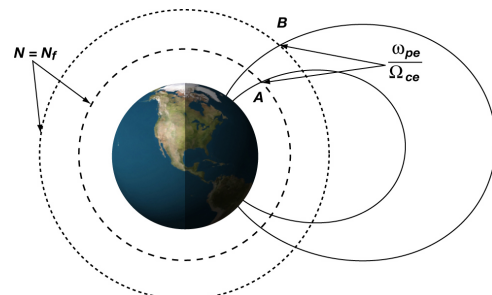
Figure 4. A schematic depicting the migration of the location of optimal wave-particle interaction region characterized by a specific electron plasma frequency-to-gyro frequency ratio, ω_{pe}/Ω_{ce}. Due to the increases of ionospheric densities and scale heights from a (dashed circle) solar minimum to a (dotted circle) solar maximum, the slot region is expected to move correspondingly to a slightly high L value as observed, and vice versa.

the expected overall increases in ionospheric densities and scale heights during solar maximum, the region having the same plasma condition as region A must migrate to region B at higher altitudes and higher latitudes in order to maintain the same $\omega_{pe}^2/\Omega_{ce}$, consistent with the observed shift of the slot between a solar minimum and a solar maximum.

[18]   One point to note from Figure 4 is that the primary regions of enhanced scattering losses, A and B, must be located off the magnetic equator (at least for quiet times) as the magnetic field strengths there only decrease with radial distances. The finite latitudinal change between A and B is a direct consequence of maintaining the same plasma density and magnetic field strength conditions in order for the optimal occurrences of the same scattering processes to form the slot in different solar cycles. In addition, the scattering losses seem to be more effective at the beginning of a rising phase of a solar cycle and are least effective at the beginning of a declining phase, as suggested by the observed long-term variations of the residual energetic electron fluxes in the slot over the solar activity cycles (Figure 3 (top)).

[19]   Finally, we need to point out that movements of the slot over the solar cycle time scale in a sense opposite to what is described in this paper has been noted previously. *Vernov et al.* [1969] analyzed multiple short-term data sets obtained by different platforms in ~1958–1965 with various threshold energies in the range of >100 keV to >1 MeV, and noted that the radiation belt gap tends to migrate to higher L as solar activity decreases. This result is clearly inconsistent with what is being reported here, although *Vernov et al.* [1969] also pointed out that "some scatter of points may be due to time variations and to the differences between electron energies measured in various experiments." The combined use of the MSQS [*Fung*, 2004a] and the long-term NOAA data sets used in the present study may be better suited for the type of investigations being reported here and therefore may provide a more accurate characterization of the solar-cycle changes of the quiet-time radiation belt slot.

5.   Conclusions

[20]   After analyzing the long-term NOAA satellite (5, 6, 7, 8, 10, 12 and 14) observations at low altitude (~850 km), we have found that the quiet-time slot region of the Earth's radiation belts exhibits an oscillatory motion in L that is connected to the solar-cycle variations. The slot is found to be located at slightly higher L (~3) during a solar maximum with a higher residual slot energetic electron fluxes (>300 keV) occurring at the end of the corresponding solar maximum. By comparison, at solar minimum, the slot is located at lower L (~2.5) and is more depleted with energetic electrons near the end of the solar minimum.

[21]   The reported findings can be understood in terms of the migrations of the enhanced precipitation loss region with the changes of ionospheric densities and scale heights between solar cycle phases. They suggest that the primary wave-particle interaction region is situated along the mid-latitude field lines and not at the magnetic equator. This supports the importance of incor-

porating wave activity distributions along the geomagnetic field lines when modeling the radiation belts [*Boscher et al.*,1997; *Fung*, 2004b].

References

Abel, B., and R. M. Thorne (1998a), Electron scattering loss in Earth's inner magnetosphere: 1. Dominant physical processes, *J. Geophys. Res.*, *103*, 2385–2396.

Abel, B., and R. M. Thorne (1998b), Elecron scattering loss in Earth's inner magnetosphere: 2. Sensitivity to model parameters, *J. Geophys. Res.*, *103*, 2397–2407.

Bortnik, J., U. S. Inan, and T. F. Bell (2002), *L* dependence of energetic electron precipitation driven by magnetospherically reflecting Whistler waves, *J. Geophys. Res.*, *107*(A8), 1150, doi:10.1029/2001JA000303.

Bortnik, J., U. S. Inan, and T. F. Bell (2003), Energy distribution and lifetime of magnetospherically reflecting Whistlers in the plasmasphere, *J. Geophys. Res.*, *108*(A5), 1199, doi:10.1029/2002JA009316.

Boscher, D., et al. (1997), Spatial distributions of the inner radiation belt electrons: A comparison between observations and radial diffusion theory predictions, *Adv. Space Res.*, *20*, 369–372.

Friedel, R. H. W., and A. Korth (1995), Long-term observations of keV ion and electron variability in the outer radiation belt from CRRES, *Geophys. Res., Lett.*, *22*, 1853–1856.

Fung, S. F. (2004a), Announcement of a "Magnetospheric-State Query System," *SPA Sect. Newsl. XI*, edited by P. Chi, AGU, Washington, D. C. (Available at ftp://igpp.ucla.edu/scratch/aguspa/volume11_2004/vol11no009.)

Fung, S. F. (2004b), Survey of current situation in radiation belt modeling, *Adv. Space Res.*, *34*, 1441–1450.

Fung, S. F., et al. (2005), Development of a magnetospheric state-based trapped radiation data base, *Adv. Space Res.*, *36*, 1984–1991, doi:10.1016/j.asr.2004.04.020.

Green, J. L., et al. (2005a), Distribution and origin of plasmaspheric plasma waves, in *Inner Magnetosphere Interactions: New Perspectives From Imaging, Geophys. Monogr. Ser.*, vol. 159, edited by J. L. Burch, M. Schulz, and H. Spence, pp. 133–136, AGU, Washington, D. C.

Green, J. L., S. Boardsen, L. Garcia, W. W. L. Taylor, S. F. Fung, and B. W. Reinisch (2005b), On the origin of Whistler mode radiation in the plasmasphere, *J. Geophys. Res.*, *110*, A03201, doi:10.1029/2004JA010495.

Imhof, W. L., et al. (1982), Coordinated measurements of slot region electron precipitation by plasmaspheric wave bands, *J. Geophys Res.*, *87*, 4418–4426.

Imhof, W. L., et al. (1986), Slot region electron precipitation by lightning, VLF chorus, and plasmaspheric hiss, *J. Geophys. Res.*, *91*, 8883–8894.

Jursa, A. S. (Ed.) (1985), *Handbook of Geophysics and the Space Environment*, pp. 9-1, 10-47–10-50, Air Force Geophys. Lab., Bedford, Mass.

Li, X., D. N. Baker, S. G. Kanekal, M. Looper, and M. Temerin (2001), Long term measurements of radiation belts by SAMPEX and their variations, *Geophys. Res. Lett.*, *28*, 3827–3830.

Lyons, L. R., and R. M. Thorne (1973), Equilibrium structure of radiation belt structure, *J. Geophys. Res.*, *78*, 2142–2149.

Lyons, L. R., and D. J. Williams (1984), *Quantitative Aspects of Magnetospheric Physics*, pp. 168–180, Springer, New York.

Miyoshi, Y. S., V. K. Jordanova, A. Morioka, and D. S. Evans (2004), Solar cycle variations of the electron radiation belts: Observations and radial diffusion simulation, *Space Weather*, *2*, S10S02, doi:10.1029/2004SW000070.

Raben, V. J., et al. (1995), TIRO/NOAA satellite space environment monitor data archive documentation: 1995 update, *NOAA Tech. Memo. ERL SEL-86*, Space Environ. Lab., Boulder, Colo.

Stix, T. H. (1992), *Waves in Plasmas*, 81 pp., Am. Inst. of Phys., New York.

Vernov, S. N., et al. (1969), Particle fluxes in the outer geomagnetic field, *Rev. Geophys.*, *7*, 257–280.

———————————

S. F. Fung, X. Shao, and L. C. Tan, Space Physics Data Facility, NASA Goddard Space Flight Center, Code 632, Greenbelt, MD 20771, USA. (shing.f.fung@nasa.gov)